Advances in Energy Research, *Vol. 7, No. 2 (2020) 147-166*
DOI: http://doi.org/10.12989/eri.2020.7.2.147

Low-grade waste heat recovery and repurposing to reduce the load on cooling towers

Shannon H. McLean[1], Jeff Chenier[2], Sari Muinonen[2], Corey A. Laamanen[1] and John A. Scott[*1]

[1]*School of Engineering, Laurentian University, 935 Ramsey Lake Road, Sudbury, ON, Canada*
[2]*Sudbury Integrated Nickel Operations (a Glencore Company), Sudbury, ON, Canada*

(Received April 13, 2020, Revised August 18, 2020, Accepted August 19, 2020)

Abstract. Industrial cooling towers are often ageing infrastructure that is expensive to maintain and operate. A novel approach is introduced in which a heat pump circuit is incorporated to reduce the load upon the towers by extracting low-grade energy from the stream sent to the towers and repurposing in on-site processing operations. To demonstrate the concept, a model was constructed, which uses industrial data on cooling towers linked to a smelter's sulphuric acid plant, to allow direct economic and environmental impact comparison between different heat recovery and repurposing scenarios. The model's results showed that implementing a heat pump system would significantly decrease annual operating costs and achieve a payback period of 3 years. In addition, overall CO_2 emissions could be reduced by 42% (430,000 kg/year) and a 5% heat load reduction on the cooling towers achieved. The concept is significant as the outcomes introduce a new way for energy intensive industrial sectors, such as mineral processing, to reduce energy consumption and improve long-term sustainable performance.

Keywords: low-grade heat recovery; heat pumps; cooling towers; energy repurposing; mineral processing; environmental sustainability

1. Introduction

Industrial low-grade waste heat within process streams, typically classified as below 100°C, is often overlooked, despite representing a source of significant energy that if recovered could enhance overall operational sustainability (Zhang *et al.* 2016, Rubio *et al.* 2020). One such opportunity may lie in cooling towers as for example, a 162 m high wet unit used to remove heat from a 940 MWe generating unit was found to reject approximately 1760 MW of heat while operating at ambient air conditions of 31.7°C (Lee 1979).

Cooling towers use air to cool process water streams through direct contact which transfers heat to the atmosphere through evaporation. The cooled process water can be then cycled back at a reduced temperature (SPX 2016, Afshari and Dehghanpour 2019). There are different types of cooling towers, including cross-flow, where the water flows vertically and the air flows

*Corresponding author, Professor, E-mail: jascott@laurentian.ca

http://www.techno-press.org/?journal=eri&subpage=7 ISSN: 2287-6316 (Print), 2287-6324 (Online)

horizontally across water, and counter-flow, where the air flows vertically upward (SPX 2016). In addition, cooling towers can be induced draft, where fans pull air through the cooling towers, or forced draft, where air is pushed by blowers located at the air inlet (SPX 2016). Natural draft cooling towers use a stack effect, allowing hot air to rise and create a draft, and thus do not require fans (Enexio 2020). An enclosure can be used to enhance cooling efficiency, as well as inlet air spray cooling to further improve cooling performance by pre-cooling the air (Afshari and Dehghanpour 2019).

Many older cooling towers are constructed from wood that requires regular replacement to avoid environmental concerns and allow for increased efficiency (Jordan 2013, CT/HX 2014). Cooling towers can also lose 20% of capacity due to defects, such as packing and nozzle blockages (Ning *et al.* 2015), and older systems are often oversized, and are more expensive to operate than smaller more efficient modern units (Hawkeye Energy Solutions 2015).

Cooling towers present, therefore, a significant opportunity for application of heat recovery systems that would both make reuse of otherwise wasted energy and also reduce the load on them, and hence operational costs (Mazzoni *et al.* 2017). That is, enhancing rather than replacing aging infrastructure with new technology, such as heat pumps (Hawkeye Energy Solutions, 2015), to recover and repurpose low-grade energy in process streams going to a cooling tower.

To investigate this possibility, we looked as a model system, a smelter's on-site ageing cooling towers linked to a plant used to capture sulphur dioxide (SO_2) emissions from ore roasting and convert them into sulphuric acid. The cooling towers used require energy to operate fans, pump the recirculating water, and replace evaporated water (Gunson 2013, Rubio-Castro *et al.* 2013). Enhanced operation of a cooling tower presents an opportunity for substantial energy cost savings (He *et al.* 2015). Reducing the load on the cooling systems through heat recovery could help significantly to reduce costs associated with energy consumption from fan operation, as well as replacement (Rubio-Castro *et al.* 2013) and general maintenance (Hawkeye Energy Solutions, 2015, Hoffman, 2019).

2. Cooling tower efficiency limitations

Aging cooling tower infrastructure can result in a loss of heat transfer efficiency due to insufficient water and air flow, as well as corrosion and scaling (Enexio 2020), and consequently an increase in maintenance costs (Tran *et al.* 2017). Furthermore as many older cooling towers are constructed from wood, leaching of preservative chemicals into the water is a major environmental concern (Jordan 2013). Wooden cooling towers have also proven to undergo rapid physical and chemical degradation due to weathering compared to most modern, steel cooling towers (Jordan 2013, Bahtiar *et al.* 2017).

Reducing the heat load through recovery on any type of cooling tower can improve energy efficiency, as well as increase operational life (Hawkeye Energy Solutions 2015, Hoffman 2019). Recovered waste heat could be then repurposed to on-site applications such as process streams, building space heating or hot water heating (Ross 2016, Woolley *et al.* 2018). Heat load reduction can also achieve decreased fan operation, which reduces wear, energy consumption, and operating costs (Baltimore Aircoil Company).

With an increase in global activities, water consumption by the mining and mineral processing industry continues to grow. As mining resources become depleted, larger volumes of water will be required for mining and mineral processing of lower quality ores, contributing to an increased

demand for water (Prosser *et al.* 2011). Industries account for approximately 20% of the total water consumption and in Western Australia, for example, water consumption within the mining sector is projected to increase from 810 to 940 GL/year by 2027 (Prosser *et al.* 2011). While a study carried out in 2015 determined that water rates went up nationally in the United States by 41% since 2010 (Hoffman 2019). As industries look to become more water and energy efficient, cooling towers without the addition of load reduction techniques, may become a less attractive option (He *et al.* 2015). Implementing strategies to reduce water consumption is key to attaining a sustainable mining industry (Gunson 2013). Therefore, in addition to improving cooling tower performance, a reduced heat load can also help through decreased water consumption.

3. Cooling tower operation

To study the impacts of recovering and repurposing on-site low-grade heat from process water going to cooling towers, we looked at towers in operation at the Sudbury Integrated Nickel Operations (Sudbury INO) smelter site in Canada. The smelter processes nickel and copper custom feeds, as well as smaller amounts of cobalt, gold, silver, platinum, and palladium (Ross, 2016). Three major sources of low-grade waste heat have been identified at the smelter: which are the (1) furnace cooling water, (2) matte granulation cooling water, and (3) acid plant cooling water. In total they represent over 60 MW of low-grade waste heat that is dissipated to the atmosphere (Ross 2016).

Within the acid plant, sulphur dioxide (SO_2) at a content of 6-7% is recovered from the off-gas of the fluidized bed concentrate roasters and is converted into sulphuric acid at an average product acid flow rate of 40 tonnes/h (Laamanen *et al.* 2014). The other off-gas that is not directed to the acid plant, undergoes a number of cleaning stages, including an electrostatic precipitator, before it is released to the environment (Ross 2016). The electrostatic precipitator is the final gas cleaning stage and consists of four operating electric heaters at a capacity of 60 kW each, plus one on standby. The overall process is illustrated in Fig. 1.

In the acid plant, a quench-condenser process is used to cool the roaster off-gas, resulting in a weak acid liquid for neutralization and disposal. Cooling tower water removes the heat from the

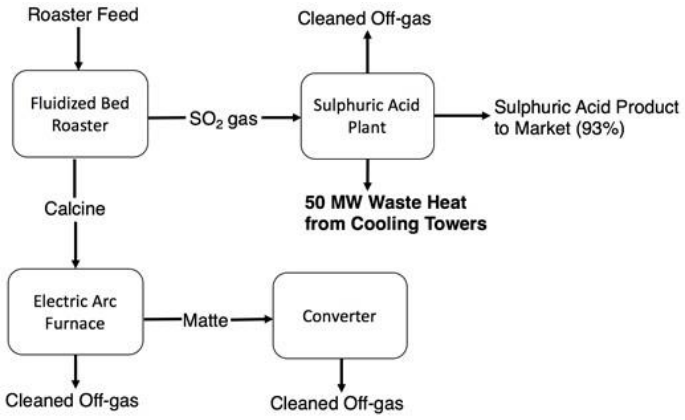

Fig. 1 Sulphuric acid production from smelter off-gas (adapted from (Laamanen *et al.* 2014))

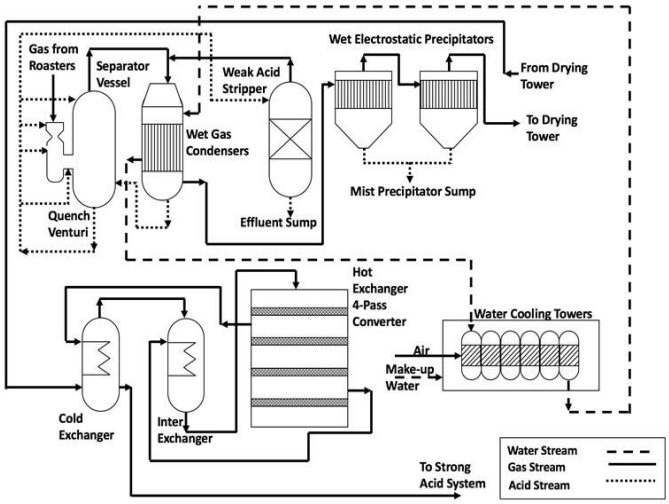

Fig. 2 Acid plant process for weak acid

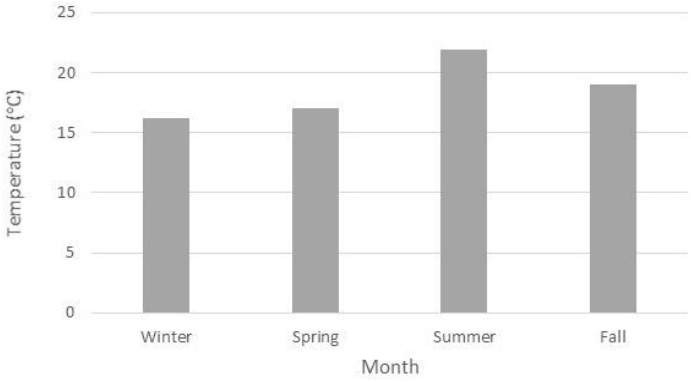

Fig. 3 Average water temperatures from the cooling towers over 2016 and 2017 (Sudbury INO 2017)

off-gas stream, and the cooled SO_2 gas is brought to the drying tower where water is removed. After this step, the SO_2 gas travels to the converter through a series of gas-gas heat exchangers. After catalytic conversion of the SO_2 to SO_3 the gas is sent to the absorbing tower before it is eventually released through the main stack. The reaction that takes place in the converter is exothermic, and heat from the process is used to preheat the incoming SO_2 gas stream. At the end of the acid plant process, the final acid product reaches its target concentration of about 93% before it is sent to storage and then sold. Cooling tower water is also used to remove heat from the acid in the drying, absorbing, and product transfer stages. The process within the plant is illustrated in Fig. 2.

An investigation was made into heat recovery from the cooling towers for repurposing within sulphuric acid production. Data from the water cooling towers was collected and used to model a number of systems to determine techniques that could be applied to recover and upgrade the low grade industrial heat in an economical manner. Typically, an upgraded temperature of around 25°C allows otherwise-waste heat to be used in repurposing applications (Miah *et al.* 2015). The

focus was on applying heat pumps as they are generally regarded as one of the better techniques to achieve this level of heat upgrade from low temperature water streams, compared to heat exchangers and the Organic Rankine cycle that typically require temperatures greater than 100°C for recovery (Rubio *et al.* 2020).

The concept is to implement a heat recovery system for the acid plant supply cooling water leaving the tower, which had an average annual temperature of 18℃, ranging from about 1℃ to 27℃ (Fig. 3). This includes operating the cooling tower fans at a decreased speed to allow the cooling water supply temperature to increase, thereby creating an opportunity for heat pumps to capture more heat and reduce the temperature back down to the required 18°C. The approach would offer additional benefits from decreasing electricity consumption by the cooling tower fans, and potentially, a reduced number of required cooling towers.

Power consumption by the cooling tower fans contribute substantially to the overall operating costs as typically required is around 0.01 kWh of energy per kWh of cooling energy (Gunson 2013). As fan power is proportional to the cube of its speed (Baltimore Aircoil Company), reducing the speed by 20% should decrease energy consumption by approximately 50%. This has been confirmed as a report described how reducing the speed of a 100 horsepower fan that operates at 1294 RPM for 2000 hours/year by 25%, reduced annual operating costs by more than 50% (Hawkeye Energy Solutions 2015).

4. On-site low-grade waste heat recovery and repurposing applications

The inlet water from the sulphuric acid plant to the cooling towers is 33℃, ranging from about 2℃ to 41℃, and is distributed equally between six separate cells, each with its own fan. The cells share a common basin where the cooled water is collected and pumped back to the acid plant. The air flow through each cell is about 680,000 m^3/h throughout the year. The average flow rate of cooling water flowing from the cooling tower is 4104 m^3/h.

The two processes chosen as potential applications for recovered waste heat were the wet electrostatic precipitator (ESP) and the weak acid stripper tower, both of which require heating in the colder months (December to April), where typical minimum ambient temperatures range from -18°C to 3°C (Weather Atlas 2020). To prevent the acid from freezing, the weak acid stripper tower employs a thermostat controlled 144 kW electric heater that turns on when the ambient air temperature drops to 5°C. The wet electrostatic precipitator (ESP) has four 60 kW electric heaters plus one on standby. The heaters run year-round and raise ambient air temperature to 100°C to provide dry purge air (1,000-2,000 m^3/hr) to the electrical insulator compartments. Maintaining the air at this temperature keeps any water in the vapour phase and prevents condensation from damaging the insulators. The annual heating demands of the weak acid (WA) stripper tower and the wet ESP are illustrated in Fig. 4.

A model was developed to assess two different configuration scenarios of heat pump systems to recover heat from the cooling tower supply water. The aim was to compare purchase and operational costs, energy consumption and overall greenhouse gas (CO_2) emissions. Scenario 1 was aimed at the maximum number of heat pumps that would be required during the colder months when the equipment heating demand is at its peak. The heat pump banks would be installed at each piece of equipment where recovered heat would be used, that is the wet electrostatic precipitator and the weak acid stripper, and the system would require the cooling water to be split and pumped to the individual heat pump banks.

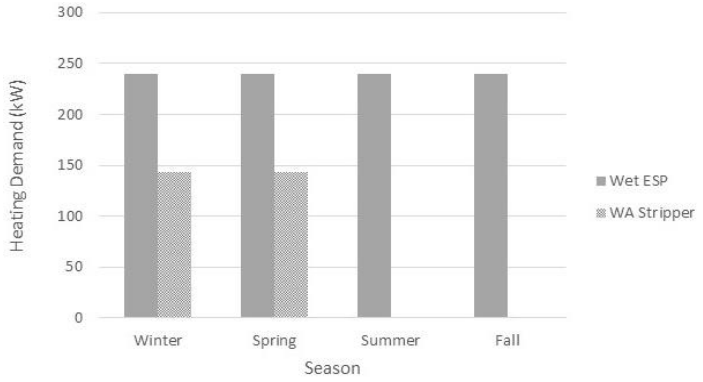

Fig. 4 Heating demands of the weak acid (WA) stripper and wet electrostatic precipitator (ESP) (Sudbury INO 2017)

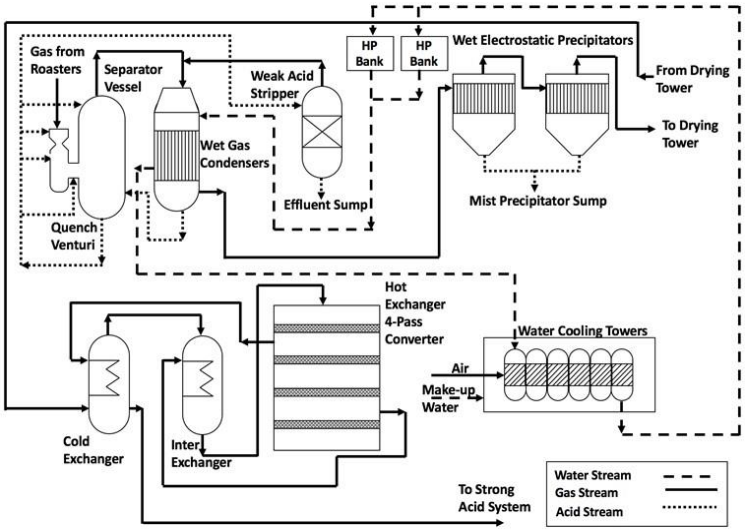

Fig. 5 Heat recovery system (HP = Heat Pump)

However, during the summer months when less heat is required, with Scenario 1, some of the heat pumps would remain idle. To avoid this idle capacity, in Scenario 2 a model was constructed that includes only the number of heat pumps required to replace the maximum number possible of year-round electric heaters of the wet electrostatic precipitator, while keeping the existing weak acid stripper heater for the winter months. A process schematic that includes the two heat pump scenarios is given in Fig. 5.

The heating scheme for each scenario uses open loop heat pumps in a parallel arrangement to allow for higher recovery efficiency as each unit would be exposed to the process water at its highest temperature (Ross 2016). Whereas an arrangement in series would result in a lower efficiency of the bank, due to the temperature drop through each individual heat pump. Water-to-air ground source heat pumps (GSHPs) were chosen due to their high capacities and low source temperature applications (Ammar *et al.* 2012, Ahmad and Prakasha 2019). These heat pump units are equipped with a blower, and allow for the captured heat to be transferred to the incoming

process air through heat exchange between the warm water and a refrigerant within the heat pump coils. The cost of this equipment is factored into the overall cost of heat pumps.

5. Heat recovery model

Pipe flow equations for heat and pressure loss were used in the model to determine the number of heat pumps required to overcome these losses and provide an efficient temperature lift. Annual costs for the heat pump systems could then be calculated from electricity consumption, as well as capital costs. The heat loss (q) that occurs from pumping water across the length of pipe to the heat pump bank during a time interval (Δt) was expressed as follows (Lienhard and Lienhard 2013), where $q\cdot$ is the heat transfer rate:

$$q = \int_0^{\Delta t} q\cdot dt \tag{1}$$

Heat transfer through the pipe (q), modelled as steady-state, can be determined from the density of the fluid (ρ), as well as the volumetric flow rate (Q), the specific heat capacity of the fluid (c_p) and the temperature change across the section of pipe ($T_{p2} - T_{p1}$):

$$q = \rho Q c_p \left(T_{p2} - T_{p1}\right) \tag{2}$$

The heat flux ($Q\cdot$) is the rate of heat transfer ($q\cdot$) per unit area (A), as represented by:

$$Q\cdot = q\cdot / A \tag{3}$$

Total thermal resistance (R_{total}) is calculated as the sum of the internal resistance to convection ($R_{interior}$), the resistance to conduction through the pipe (R_{pipe}), the resistance through the insulation ($R_{insulator}$), and the resistance to external convection ($R_{exterior}$). The thermal conductivity (k) of a steel pipe, 45 Wm^{-1} K^{-1}, and that of the fiberglass insulation, 0.04 Wm^{-1} K^{-1} (Ross 2016), are required to determine resistance through the pipe and resistance through the insulation, respectfully. The Fourier equation was used for steady-state conduction and assuming thermal conductivity is constant, it can be represented as follows (Sukhatme 2005):

$$\begin{gathered} q\cdot = -kA\,(dT/dr) \\ A = 2\pi rL \end{gathered} \tag{4}$$

Eq. (6) results from integrating the Fourier equation, where the temperature difference across the layer is represented by T_1–T_2. After integration, the thermal resistance against heat conduction of the pipe layer is determined (Lienhard and Lienhard 2013) in Eq. (8), where r_2 and r_1 are the outer and inner radius of the pipe, respectively.

$$\int_{r_1}^{r_2} (q\cdot/A)\, dr = -\int_{T_1}^{T_2} k dT \tag{5}$$

$$\int_{r_1}^{r_2} (q\cdot/A)\, dr = -\int_{T_1}^{T_2} k dT \tag{6}$$

$$q^{\cdot} = \frac{T_1 - T_2}{R} \tag{7}$$

$$R = \frac{\ln (r_2/r_1)}{2\pi kL} \tag{8}$$

The heat transfer across the fluid/solid interface comes from Newton's law of cooling (Sukhatme 2005), where h is the heat transfer coefficient, T_s is the temperature of the surface, and T_a is the temperature of ambient air. This is used to determine the thermal resistance of the surface against heat convection (R_{conv}) written as Eq. (10).

$$q^{\cdot} = hA(T_s - T_a) \tag{9}$$

$$R_{conv} = \frac{1}{hA} \tag{10}$$

In a pipe, interior and exterior resistance due to convection are represented below with Eq. (11) and Eq. (12), respectively. Thermal resistance against heat conduction through the pipe, Eq. (13), and thermal resistance through insulation, Eq. (14), are shown. In Eq. (14), the outer pipe radius (r_2) and the outer insulation radius (r_3) are used to determine the thermal resistance through insulation.

$$R_{interior} = \frac{1}{h_1 A_1} \tag{11}$$

$$R_{exterior} = \frac{1}{h_2 A_2} \tag{12}$$

$$R_{pipe} = \frac{\ln (r_2/r_1)}{2\pi k_{pipe} L} \tag{13}$$

$$R_{insulation} = \frac{\ln (r_3/r_2)}{2\pi k_{insulation} L} \tag{14}$$

The total resistance is calculated as the sum of the resistance equations:

$$R_{total} = R_{interior} + R_{pipe} + R_{insulation} + R_{exterior} \tag{15}$$

With values for total thermal resistance, ambient air temperature and process water temperature (T_{water}), the overall heat loss to ambient air from the process water travelling through a length of pipe (q) can be determined:

$$q = \frac{T_a - T_{water}}{R_{interior} + R_{pipe} + R_{insulation} + R_{exterior}} \tag{16}$$

$$q = \frac{T_a - T_{water}}{\frac{1}{Nu\,(k/D)\,\pi DL} + \frac{\ln (r_2/r_1)}{2\pi k_{pipe} L} + \frac{\ln (r_3/r_2)}{2\pi k_{insulation} L}} \tag{17}$$

$$h = \frac{Nuk}{D} \tag{18}$$

To solve for the convection heat transfer coefficient (h), Eq. (18), the Nusselt number (Nu) must be first calculated. The Nusselt number represents the convection heat transfer that occurs at the surface, and is a ratio of thermal energy convected to thermal energy conducted within the fluid (Nuclear Power, 2019c). For fully developed turbulent flow in a pipe, the Nusselt number may be obtained from the Dittus-Boelter expression, Eq. (20) (Nuclear Power, 2019c), where *Re* is the Reynolds number and *Pr* is the Prandtl number:

$$Nu = f(Re, \Pr) \tag{19}$$

$$Nu = \frac{q_{conv}}{q_{cond}} = \frac{h\Delta T}{k(\Delta T/L)} = \frac{hL}{k} \tag{20}$$

$$Nu = 0.023 Re^{0.8} Pr^{0.4} \tag{21}$$

Application of Eq. (21) is valid under the following conditions (Nuclear Power 2019c):

$$0.6 \leq Pr \leq 160$$
$$Re > 10\,000$$
$$L/D > 10$$

The Prandtl number represents the ratio of momentum diffusivity to thermal diffusivity (Nuclear Power 2019a), and is approximated by Eq. (22), where v is the kinematic viscosity of the fluid, α is the thermal diffusivity, and μ is the fluid viscosity.

$$\Pr = v/\alpha = \frac{(\mu/\rho)}{(\frac{k}{C_p/\rho})} = \frac{\mu C_p}{k} \tag{22}$$

To determine the additional power requirements needed to pump the cooling water to the heat pump bank (W_{pump}), the pressure drop across the length of the pipe can be calculated from volumetric flow rate, pressure loss (ΔP) and efficiency (E) (Lienhard and Lienhard 2013):

$$W_{pump} = \frac{Q\Delta P}{E} \tag{23}$$

The Darcy-Weisbach equation (Eq. (24)) was used to determine head loss or pressure loss for a length of pipe due to friction, from the average velocity of the fluid flow (u) (Lienhard and Lienhard, 2013). The pressure drop across the length of the pipe can be calculated as the sum of the major losses (ΔP_{major}) in pipe flow due to friction, with a friction factor f, and minor losses (ΔP_{minor}) due to tees and elbows along the piping route, written as Eq. (24) and Eq. (25), respectively. The minor loss coefficient for pipe components (K_L) and the dynamic pressure in fluid flow can be used to determine the pressure drop due to minor losses, Eq. (25).

$$\Delta P_{major} = f \frac{L}{D} \frac{\rho u^2}{2} \tag{24}$$

$$\Delta P_{minor} = K_L P_d = K_L \frac{\rho u^2}{2} \tag{25}$$

$$K_L = f(L/D) \tag{26}$$

The following denotes the total pressure drop as the sum of major and minor losses (Munson *et al.* 2013):

$$\Delta P_{Total} = f \frac{L}{D} \frac{\rho u^2}{2} + \sum K_L \frac{\rho u^2}{2} \tag{27}$$

The major and minor losses can also be expressed as equivalent pipe length (*Le*) to solve for head loss (h_L) (Bansal, 2005):

$$h_L = f(L/D + \sum (Le/D)) \frac{u^2}{2g} \tag{28}$$

$$h_L = (f\,(L/D) + \sum K_L) \frac{u^2}{2g} \tag{29}$$

The Darcy-Weisbach equation can be used to solve for head loss in terms of volumetric flow rate in a pipe, Eq. (32), by substituting the following (Bansal 2005):

$$u^2 = Q^2/A_w^2 \tag{30}$$

$$A_w^2 = (\frac{\pi D^2}{4})^2 \tag{31}$$

$$h_L = \frac{8 f L Q^2}{g \pi^2 D^5} \tag{32}$$

The Swamee-Jain equation is an approximation that is widely used to solve the Darcy friction factor for turbulent flow in smooth and rough pipes (Kiijarvi 2011), where $\frac{\varepsilon}{D}$ represents the relative pipe roughness:

$$f = \frac{0.25}{(log_{10}(\frac{\varepsilon/D}{3.7} + (5.74/Re^{0.9})))^2} \tag{33}$$

The Reynolds number (*Re*), which represents the ratio of inertial forces to viscous forces, is used to predict if a flow will be laminar or turbulent (Nuclear Power, 2019b). Eq. (33) is valid for a Reynolds number between 2300 and 4000, ~2300<*Re*<~4000.

$$Re = \frac{\rho u D}{\mu} = \frac{u D}{\upsilon} \tag{34}$$

Substituting the Reynolds number, expressed as Eq. (34), into Eq. (33) yields the pressure loss

along a given length of pipe in terms of the Darcy friction factor:

$$\Delta P = \frac{0.25}{(log_{10}(\frac{\varepsilon/D}{3.7} + \frac{5.74}{\left(\frac{uD}{\upsilon}\right)^{0.9}}))^2} \frac{L}{D} \frac{\rho u^2}{2} \tag{35}$$

The temperature of the process water entering the heat pump bank ($T_{w,in}$) was determined from the water temperature drop across the length of pipe:

$$T_{w,in} = T_{water} - \frac{q}{QC_p\rho} \tag{36}$$

As fan horsepower (*HP*) will vary by the cube of the ratio of fan speed (Axair Fans 2018), to determine the power savings by reducing the speed of the cooling tower fans (*RPM*), the following relation was used:

$$(RPM_1/RPM_2)^3 = HP_1/HP_2 \tag{37}$$

The speed of the fan and the airflow are proportional and, therefore, decreasing the speed of the cooling tower fans will result in a reduced air flow through the cooling tower cells. The revised speed of fans (RPM_2) can be determined by relating the original air flow (CFM_1), the new desired air flow (CFM_2) and the original speed of the fans (RPM_1) (Axair Fans 2018):

$$RPM_1/RPM_2 = CFM_1/CFM_2 \tag{38}$$

Water temperatures and flow rate data were collected for each day of the year, along with ambient air temperature and heating requirements for each month. MATLAB (Matlab 2014) was then used to create a model to determine the overall annual operating costs of the two heat pump scenarios, as well as the number of heat pumps required in each bank for each system.

In addition to the heat and pressure losses through the piping, the number of heat pumps required was calculated based on the capacity of each individual heat pump, and the required heating of the wet electrostatic precipitator and the weak acid stripper. A commonly used performance indicator for a heat pump cycle is the coefficient of performance (COP) (Ataei *et al.* 2016, Yang and Lee 2020). For heating applications, the COP is the ratio of heat delivered from the heat pump to the work input required from all external sources, such as electricity to run the compressors (Gudjonsdottir *et al.* 2017). Therefore, a higher COP indicates a better efficiency (Antwan and Maree 2010).

In Scenario 1, the number of heat pumps required to supply heat to both the weak acid stripper and the wet electrostatic precipitator throughout the winter months was determined. Operating costs for both scenarios included electricity to run the heat pumps, as well as the power to pump water to the heat pump banks and back to the process cooling lines. In addition, for Scenario 2 were the costs associated with using electric heaters for the weak acid stripper during the winter months.

Capital costs of the heat pump systems (*C*) were determined in order to calculate a payback period. The capital cost of an individual heat pump as a function of capacity (*HC*) can be approximated by (Staffell *et al.* 2012):

$$C = 1.64HC(200 + (4750/HC^{1.25})) \tag{39}$$

The equation was verified for use in the model by applying current capital cost and heating

capacity data for water-to-air heat pumps acquired from various vendors. In addition, the approximation was made applicable to 2018 Canadian dollars by employing the appropriate exchange rate and inflation. Along with the cost of purchasing the heat pumps, the capital costs must also include those for additional piping and insulation. The cost of piping was calculated based on the unit capital cost for steel pipe and fiberglass insulation of approximately $100/m and $30/m, respectively (Ross, 2016). Since the aim of the developed model was to perform a comparative cost analysis between the proposed heat pump system and the electric heaters currently in place, estimated maintenance costs were not included in annual cost calculations, as they were assumed to be similar for both systems.

The total annual savings in operating costs for both scenarios investigated were calculated and used to determine the payback period with an assumed heat pump life of 20 years (Staffell *et al.* 2012). Any operational cost savings were determined by comparing electricity consumption by the heat pump system and by the current electric heater arrangement. The total capital costs of the heat pump system were annuitized by using Eq. (40), where PV represents the present value, i is the hurdle rate, and n is the number of years. The present value is calculated using Eq. (41), where c_1 represents the cash flow, and r is the rate of return.

$$AV = PV\frac{i(i+1)^n}{(i+1)^n - 1} \tag{40}$$

$$PV = \frac{C_1}{(1+r)^n} \tag{41}$$

6. Results and discussion

(1)*Scenario 1*

The simulations for Scenario 1 showed potential as an economically feasible system to replace the current electric heaters. The temperature dependent COP of each heat pump was calculated within the model using the varying temperature values of the cooling water entering the heat pump bank. With the heat pump efficiencies consisting of a COP ranging from 5.2 to 5.6, and accounting for heat losses across the pipe network to the equipment, replacing the electric heaters of both units of equipment would allow for a heat load reduction of the cooling towers by 7% in the winter, and 5% in the summer.

The temperature of heated air supplied by the heat pumps must be appropriate for the potential applications chosen. For the weak acid stripper, the system was designed to be sufficient to raise the temperature of ambient air from as low as -40°C to the required output minimum of 5°C. For the wet electrostatic precipitator, the heat pump bank selected could raise the ambient air temperature to 85°C, with a 10kW electric heater then employed on the combined outflows to produce a final air temperature of 100°C.

To determine an efficient heat pump brand and model for this application, two different heat pump brands were chosen, each comparing three different commercially available heat pumps. The heat pump displaying the best results for reduced operating costs in Scenario 1 was selected for further investigation, including comparing operating costs and CO_2 emissions of both scenarios. The temperature change of the process water leaving the heat pump bank, along with the

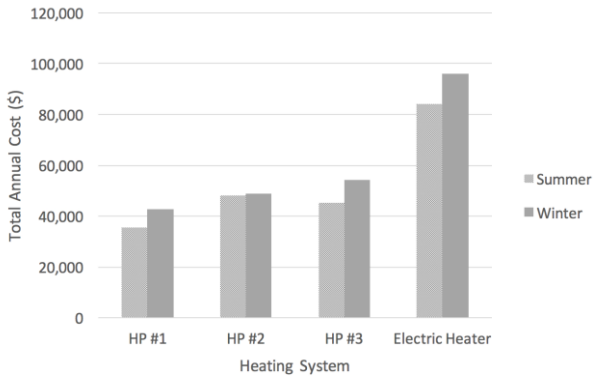

Fig. 2 Total annual operating costs of selected heating systems for Scenario 1

Table 1 Number of heat pumps and total annual operating costs of selected heating systems for Scenario 1

Heating System	Number of pumps in bank	Number of Operating Pumps During Summer	Annual Cost ($)
Electric Heaters	N/A	N/A	180,000
Heat Pump #1	5	3	77,000
Heat Pump #2	7	5	96,000
Heat Pump #3	5	3	99,000

temperature dependent COP for the heat pumps from various suppliers were determined and used in the model. Operating costs (shown in Canadian dollars) were obtained using October 2019 costs of electricity ($0.0685/kWh) where the smelter is located (Hydro One 2019).

The heat pump units investigated were compared against the current electric heater system. The capacity and power input of each heat pump chosen are presented in Table 1.

The number of heat pumps required in a bank for each system was determined and is presented in Table 1. The operating costs calculated for each heat pump system include those associated with pumping water to and from the heat pump bank, as well as those to power the required number of heat pump units and remaining electric heater of the mist precipitator. In Fig. 6, the annual operating costs for each heat pump systems chosen are compared against the existing electric heater system (EH). Additional costs of running the single electric heater for the mist precipitator are added onto the total annual costs of the heat pump system.

The results of the model, illustrated in Table 1, indicate that for this scenario the most efficient heat pump system results from using Heat Pump #1. Therefore, Heat Pump #1 is used for further investigation in comparing annual operating costs and CO_2 emissions from Scenario 1 against Scenario 2. Capital costs for this system were calculated to be $334,000 while total annual operating costs were reduced by 57% from the current heating system in place. The capital costs of the heat pump systems were calculated based on the capacity of the individual heat pump units used. The approximation is shown as Eq. (39). These costs vary for each heat pump system modelled, since the heat pump brands investigated each have different capacities for varying water temperatures. The capital costs also included costs of purchasing and installing additional piping.

As CO_2 is released during the combustion of fossil fuels to produce electricity (United States Environmental Protection Agency 2018), electricity use is, therefore, related to greenhouse gas

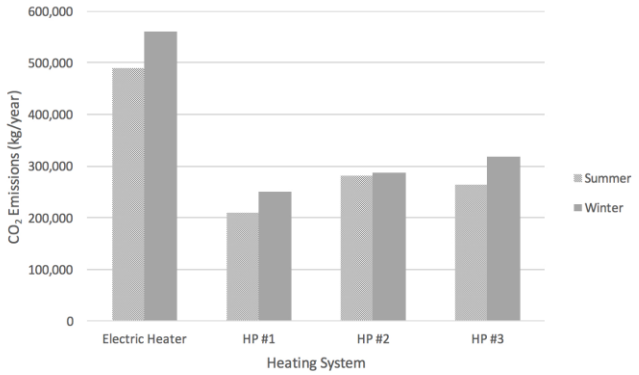

Fig. 7 Annual CO2 emissions from Ontario electricity supply associated with the heating systems selected for Scenario 1

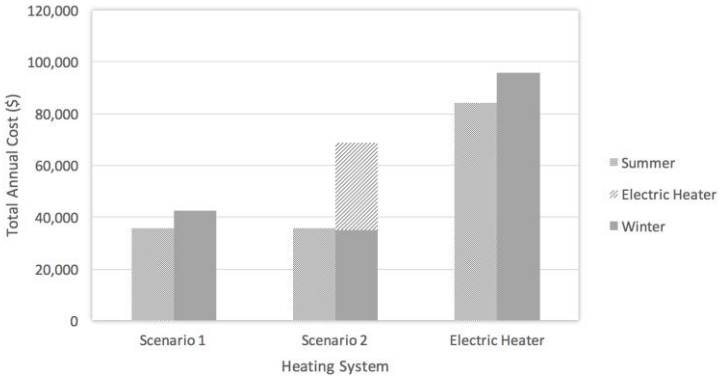

Fig. 8 Total annual operating costs of selected heating systems using Heat Pump #1

emissions. The annual emissions calculated for each system was based on 0.4 kg CO_2/kWh of electricity consumption where the smelter is located (Williams *et al.* 2017). The CO_2 emissions associated with each modeled heat pump system were calculated based on overall electricity consumption by Scenario 1 and compared against the emissions released by the current electric heaters (Fig. 7).

(2) *Scenario 2*

In Scenario 2, the three heat pumps needed are linked to the year-round heat demand of only the wet electrostatic precipitator. That is, the electric heaters already in place for the weak acid stripper would remain in place for operation when required over the winter months. Scenario 2 allows, therefore, for elimination of idle heat pumps during the warmer summer months, when no heat is required by the weak acid stripper.

Implementing Scenario 2 would allow for a year-round 5% reduction in the heat load of the cooling towers. The number of heat pumps required in a bank for the heat recovery system in both scenarios is illustrated in Table 2. In Scenario 2, as the existing weak acid stripper electric heater is in operation during the winter months, less heat pumps will be in operation when compared to Scenario 1.

A comparison of both scenarios using Heat Pump #1, as well as the current electric heater

Table 2 Number of heat pumps and total annual operating costs of selected heating systems

Heating System	# Pumps in bank	# Operating Pumps During Summer Months	Annual Cost ($)
Electric Heaters	N/A	N/A	180,000
Scenario 1	5	3	77,000
Scenario 2	3	3	105,000

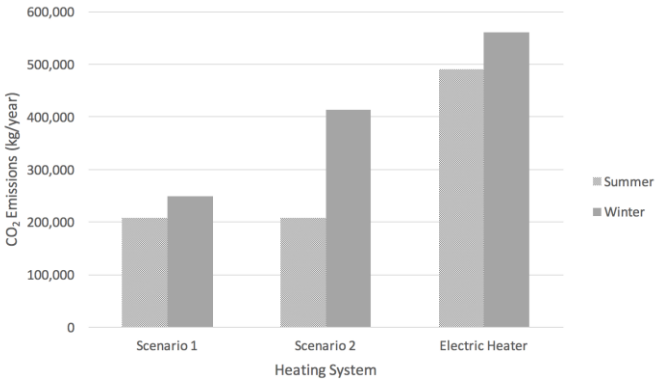

Fig. 3 Annual CO_2 emissions from Ontario electricity supply associated with the heating systems selected using Heat Pump #1

system in place, is illustrated in Fig. 8. Additional costs of running this electric heater in the winter are added onto the total annual costs of the heat pump system in Scenario 2.

As a greater number of heat pumps are required for Scenario 1 then capital costs are higher than those of Scenario 2. That is, keeping the electric heater in place for the weak acid stripper (Scenario 2) will result in a reduction in capital costs. The results of the model indicated that the most efficient scenario and heat pump system would be Scenario 2 when using Heat Pump #1 units. Capital costs for Scenario 2 were calculated to be $184,000 and with total annual operating costs at $105,000 for both the heat pump system and the existing electric heater. This would require three heat pumps to be operated at full capacity throughout the year, resulting in a 42% reduction in operating costs from the current heating system in place. Pumping water directly to the wet electrostatic precipitator heat pump bank, while using the electric heater already in place for the weak acid stripper in the winter, would result in the lowest payback period of approximately three years. Therefore, Scenario 2 was selected as the most economically viable solution.

In both Scenarios 1 and 2, the heat pump systems investigated resulted in an overall reduction in electricity consumption. Not only does this offer a potential economically viable solution for waste heat application, but it also allows for a more environmentally sustainable operation with a reduction in CO_2 emissions due to electricity generation. Annual CO_2 emissions released with the heating systems of Scenario 2, illustrated in Fig. 9, resulted in a 42% reduction from the original heating system. It was established that the system with the least CO_2 emissions would be Heat Pump #1 used in Scenario 1, releasing approximately 457,000 kg/year, and thus was selected as the most environmentally sustainable design. This would result in a CO_2 reduction of about 593,000 kg annually. However, the implementation of this system would result in a payback

period of approximately 4 years, and thus is not the most economically feasible option.

One of the major benefits of reducing the heat load of the cooling towers is the opportunity to reduce the number of cooling towers required within the acid plant. Although this heat recovery design allowed for a heat load reduction ranging from 5% to 7%, a cooling tower load reduction of at least 17% would allow for a reduction of cooling towers in this case from 6 to 5 tower cells at this particular smelter site. This would be beneficial for smelter sites with aging cooling towers scheduled to be replaced, or new sites in the start-up phase, looking to install fewer cooling towers with an integrated heat recovery system. Minimizing cooling tower units will also reduce costs associated with energy consumption and general maintenance costs (Rubio-Castro *et al.* 2013). For example, according to one study's projections, eliminating the need for three cooling tower units scheduled to be replaced could result in savings of $1,085,000 in capital (Young, 2018). In addition to reducing construction costs associated with replacing aging infrastructure, reducing the number of cooling towers required can also aid in minimizing fan operational costs. At the acid plant investigated, eliminating a cooling tower unit would result in annual cost savings of over $44,000 from fan operation alone.

In this case study, a reduced heat load could allow for an improvement in energy efficiency, as well as an increase in the life of the existing towers. Reduced fan operation can be achieved, minimizing wear and operating costs. Reducing the fan speed of all 6 cooling tower fans by 10% results in a new airflow of approximately 3,670,000 m^3/h through the 6 cells of the cooling tower. The power of the fans decreases from 447 kW to about 326 kW, which allows for a savings in fan operating costs of about $72,000 per year, during peak heating demand of equipment in winter months, when heat pumps operate at capacity.

7. Conclusions

There is potential in industry for reducing emissions related to heating applications through recovery of low-grade waste heat. This has been demonstrated by a novel use of heat pumps to recover waste heat from water streams sent to cooling towers and repurpose to replace on-site process stream heaters. The model developed allows for various heat pump and on-site repurposing scenarios, comparative predictions in energy savings, operating costs and reduced CO_2 emissions.

It was determined that the payback period was approximately three years. Furthermore, reducing the heat load on the cooling towers would allow for a further improvement in energy efficiency from lowering fan power consumption, as well as overall operating and maintenance costs. A reduction in the number of cooling towers required can be also achieved due to a reduced heat load, an approach of significant benefit to sites with aging cooling towers requiring major refurbishment or replacement. The concepts introduced are, therefore, significant as they introduce new ways for the mining and other energy intensive industrial sectors to make much better use of resources and improve their long-term sustainable performance.

Acknowledgments

This work was supported by the Mitacs Accelerate program and the National Science and Research Council (NSERC).

References

Afshari, F. and Dehghanpour, H. (2019), "A review study on cooling towers; types, performance and application", *ALKU J. Sci*., 1-10.

Ahmad, S.N. and Prakasha, O. (2019), "Experimental exergy assessment of ground source heat pump system", *Adv. Energy Res*., **6**(2), 161-172. https://doi.org/10.12989/eri.2019.6.2.161.

Ammar, Y., Joyce, S., Norman, R., Wang, Y. and Roskilly, A.P. (2012), "Low grade thermal energy sources and uses from the process industry in the UK", *Appl. Energy*, **89**(1), 3-20. https://doi.org/10.1016/j.apenergy.2011.06.003.

Antwan, N.F. and Maree, I.E. (2010), "The efficiency of geothermal heat pumps with vertical ground heat exchangers: A simulation under Iraqi conditions", *Proceedings of the ASME 2010 10th Biennial Conference on Engineering Systems Design and Analysis, ESDA 2010*, Istanbul, Turkey, December.

Ataei, A., Hemmatabady, H. and Nobakht, S.Y. (2016), "Hybrid thermal seasonal storage and solar assisted geothermal heat pump systems for greenhouses", *Adv. Energy Res*., **4**(1), 87-106. https://doi.org/10.12989/eri.2016.4.1.087.

Axair Fans (2018), Understanding the Basic Fan Laws; United Kingdom. https://www.axair-fans.co.uk/news/applications/understanding-basic-fan-laws.

Bahtiar, E., Nugroho, N., Hermawan, D., Wirawan, W., Sari, R., Rahman, M. and Sidik, M. (2017), "Wood deterioration of cooling tower structure at geothermal power plant", *Asian J. Appl. Sci*., **10**, 79-87. https://doi.org/10.3923/ajaps.2017.79.87.

Baltimore Aircoil Company (n.d.), Strategies to Reduce Energy and Lower Operating Costs; BAC Technical Resource. http://www.baltimoreaircoil.com/english/resource-library/file/1684.

Bansal, R.K. (2005), *A Textbook of Fluid Mechanics*, Firewall Media, India.

CT/HX (2014), Cooling Tower Repair and Refurbishment. http://www.cthx.com/services/cooling-towers.

Enexio (2020), Natural Draft Cooling Towers, Germany. https://www.enexio.com/cooling-solutions/wet-cooling-towers/natural-draft-cooling-towers.

Gudjonsdottir, V., Infante Ferreira, C.A., Rexwinkel, G. and Kiss, A.A. (2017), "Enhanced performance of wet compression-resorption heat pumps by using NH 3 -CO 2 -H 2 O as working fluid", *Energy*, **124**, 531-542. https://doi.org/10.1016/j.energy.2017.02.051.

Gunson, A.J. (2013), "Quantifying, reducing and improving mine water use", Ph.D. Dissertation, University of British Columbia, Vancouver, Canada.

Hawkeye Energy Solutions (2015), Energy Efficiency. https://www.hawkeye-es.com/energy-efficiency.

He, S., Gurgenci, H., Guan, Z., Huang, X. and Lucas, M. (2015), "A review of wetted media with potential application in the pre-cooling of natural draft dry cooling towers", *Renew. Sust. Energy Rev*., **44**, 407-422. https://doi.org/10.1016/j.rser.2014.12.037.

Hoffman, H.W. (2019), Water Efficiency, Facilitiesnet, U.S.A. https://www.facilitiesnet.com/green/article/As-Water-Rates-Rise-Efficiency-More-Important-Especially-For-Cooling-Towers--16525.

Hydro One (2019), Electricity Pricing and Costs, Canada. https://www.hydroone.com:443/rates-and-billing/rates-and-charges/electricity-pricing-and-costs.

Jordan, S. (2013), Cooling Tower Fundamentals: The Evolution of Wooden Cooling Towers; Midwest Cooling Towers. https://midwesttowers.com/cooling-tower-fundamentals-the-evolution-of-wooden-cooling-towers.

Kiijarvi, J. (2011), "Darcy friction factor formulae in turbulent pipe flow", Research Report No. 110727; Lunowa, Finland.

Laamanen, C.A., Shang, H., Ross, G.M. and Scott, J.A. (2014), "A model for utilizing industrial off-gas to support microalgae cultivation for biodiesel in cold climates", *Energ. Convers. Manage*., **88**, 476-483. https://doi.org/10.1016/j.enconman.2014.08.047.

Lee, J. (1979), "Potential weather modification caused by waste heat release from large dry cooling towers", *J. Heat Transfer*, **101**, 164. https://doi.org/10.1115/1.3450909.

Lienhard, J.H. and Lienhard, J.H. IV (2013), *A Heat Transfer Textbook*, Third Edition, Courier Corporation, North Chelmsford, Massachusetts, U.S.A.

MATLAB 2014b (2014), *The MathWorks, Inc*, Massachusetts, U.S.A.

Mazzoni, S., Arreola, M.J. and Romangoli, A. (2017), "Innovative organic rankine arrangements for water savings in waste heat recovery applications", *Energy Procedia*, **143**, 361-366. https://doi.org/10.1016/j.egypro.2017.12.697.

Miah, J.H., Griffiths, A., McNeill, R., Poonaji, I., Martin, R., Leiser, A., Morse, S., Yang, A. and Sadhukhan, J. (2015), "Maximising the recovery of low grade heat: An integrated heat integration framework incorporating heat pump intervention for simple and complex factories", *Appl. Energy*, **160**, 172-184. https://doi.org/10.1016/j.apenergy.2015.09.032.

Munson, B., Okiishi, T., Huebsch, W. and Rothmayer, A. (2013), *Fundamentals of Fluid Mechanics*, 7th Edition, Wiley, U.S.A.

Ning, T., Chong, D., Jia, M., Wang, J. and Yan, J. (2015), "Experimental investigation on the performance of wet cooling towers with defects in power plants", *Appl. Therm. Eng.*, **78**, 228-235. https://doi.org/10.1016/j.applthermaleng.2014.12.032.

Nuclear Power (2019a), Prandtl Number Formula, https://www.nuclear-power.net/nuclear-engineering/heat-transfer/introduction-to-heat-transfer/characteristic-numbers/what-is-prandtl-number/prandtl-number-formula.

Nuclear Power (2019b), Reynolds Number. https://www.nuclear-power.net/nuclear-engineering/fluid-dynamics/reynolds-number.

Nuclear Power (2019c), What is Nusselt Number. https://www.nuclear-power.net/nuclear-engineering/heat-transfer/introduction-to-heat-transfer/characteristic-numbers/what-is-nusselt-number.

Prosser, I., Wolf, L. and Littleboy, A. (2011), *Water: Science and Solutions for Australia*, CSIRO Publishing, Australia.

Ross, I.M. (2016), "Employing heat pumps to recover low grade industrial thermal resources for space heating and cooling", M.A.Sc. Dissertaion, Laurentian University, Sudbury, Canada.

Rubio-Castro, E., Serna-González, M., Ponce-Ortega, J.M. and El-Halwagi, M.M. (2013), "Synthesis of cooling water systems with multiple cooling towers", *Appl. Therm. Eng.*, **50**, 957-974. https://doi.org/10.1016/j.applthermaleng.2012.06.015.

Rubio, C.L., García-Alcaraz, J.L., Martínez-Cámara, E., Latorre-Biel, J.I., Jiménez-Macías, E. and Blanco-Fernández, J. (2020), "Replacement of electric resistive space heating by a geothermal heat pump in a residential application–Environmental amortisation", *Sust. Energy Technol. Assess.*, **37**. https://doi.org/10.1016/j.seta.2019.100567.

SPX (2016), What is a Cooling Tower, SPX Cooling Technologies. https://spxcooling.com/coolingtowers/ (accessed 1.15.20).

Staffell, I., Brett, D., Brandon, N. and Hawkes, A. (2012), "A review of domestic heat pumps", *Energy Environ. Sci.*, **5**(11), 9291-9306. https://doi.org/10.1039/c2ee22653g.

Sudbury INO (2017), Personal Communication, Ontario, Canada.

Sukhatme, S.P. (2005), *A Textbook on Heat Transfer*, Fourth Edition, Universities Press, India.

Tran, N.C., Toulemonde, C., Beaudouin, F., Meuwisse, C., Schmitt, N., El-Yazidi, A., Courtois, A., Genest, Y. and Moriceau, S. (2017), "Innovative methodology of ranking cooling towers based on structural safety margin", *Proceedings of the 2017 25th International Conference on Nuclear Engineering*, Shanghai, China, July.

United States Environmental Protection Agency (2018), Greenhouse Gas Emissions. https://www.epa.gov/ghgemissions/sources-greenhouse-gas-emissions.

Weather Atlas (2020), Monthly Weather Forecast and Climate, Sudbury, Canada. https://www.weather-ca.com/en/canada/sudbury-climate.

Williams, M., Frankowski, C. and Allen, G. (2017), "Measuring up to global warming", Research Report No. 1602202, RWDI, Toronto, Canada.

Woolley, E., Luo, Y. and Simeone, A. (2018), "Industrial waste heat recovery: A systematic approach", *Sust. Energy Technol. Assess.*, **29**, 50-59. https://doi.org/10.1016/j.seta.2018.07.001.

Yang, S. and Lee, S.B. (2020), "Dynamic thermal analysis of a residential ground-source heat pump", *Sust. Energy Technol. Assess.*, **37**, 100608. https://doi.org/10.1016/j.seta.2019.100608.
Young, D. (2018), "Cooling towers replacement at enercare centre", Research Report No. 8.10, W.S. Nicholls Construction Inc., Toronto, Canada.
Zhang, J., Zhang, H.H., He, Y.L. and Tao, W.Q. (2016), "A comprehensive review on advances and applications of industrial heat pumps based on the practices in China", *Appl. Energy*, **178**, 800-825. https://doi.org/10.1016/j.apenergy.2016.06.049.

CC

Nomenclature

Symbol	Description	Nu	Nusselt number
α	thermal diffusivity (m^2/s)	ρ	density (kg/m^3)
A	area of surface (m^2)	ΔP	change in pressure (Pa)
A_1	area of interior surface exposed to convection (m^2)	Pd	dynamic pressure in fluid flow (Pa)
A_2	area of exterior surface exposed to convection (m^2)	Pr	Prandtl number
AV	annual value ($/yr)	PV	present value ($)
A_w	cross-sectional wetted area (m^2)	q	heat transfer (W)
C	capital costs of heat pumps ($)	$q\cdot$	heat transfer rate (W/s)
C_1	cash flow ($)	Q	volumetric flow rate (m^3/s)
C_p	specific heat capacity (J/kgK)	$Q\cdot$	heat flux (W/m^2)
CFM_1	initial air flow through cooling tower (CFM)	r	rate of return
CFM_2	reduced air flow through cooling tower (CFM)	r_1	inner radius of pipe (m)
D	inner diameter of pipe (m)	r_2	outer radius of pipe (m)
E	Efficiency of pump	r_3	outer radius of insulation (m)
ε/D	relative pipe roughness	R	thermal resistance (K/W)
f	Darcy friction factor	Re	Reynolds number
g	acceleration due to gravity (m/s^2)	RPM_1	initial fan speed (RPM)
h	heat transfer coefficient (W/m^2K)	RPM_2	reduced fan speed (RPM)
h_1	heat transfer coefficient inside pipe (W/m^2K)	Δt	time interval (s)
h_2	heat transfer coefficient outside pipe (W/m^2K)	ΔT	temperature change (K)
h_L	head loss (m)	T_1	temperature of inner surface of pipe (K)
HC	capacity of single heat pump (kW)	T_2	temperature of outer surface of pipe (K)
HP_1	initial fan power (HP)	T_a	ambient air temperature (K)
HP_2	reduced fan power (HP)	T_{p1}	temperature of water at initial section of pipe (K)
i	hurdle rate	T_{p2}	temperature of water at final section of pipe (K)

$\boldsymbol{k}$	thermal conductivity (W/mK)	T_s	temperature of surface (K)
$\boldsymbol{k_{insulation}}$	thermal conductivity of insulation (W/mK)	$T_{w,in}$	temperature of process water entering heat pump bank (K)
$\boldsymbol{k_{pipe}}$	thermal conductivity of pipe (W/mK)	T_{water}	initial process water temperature leaving cooling towers (K)
$\boldsymbol{K_L}$	minor loss coefficient for pipe components	μ	dynamic viscosity (Ns/m^2)
$\boldsymbol{L}$	length of pipe (m)	u	velocity of fluid flow (m/s)
$\boldsymbol{L_e}$	equivalent length (m)	v	kinematic viscosity (m^2/s)
$\boldsymbol{n}$	number of years	W_{pump}	pumping work (W)